Requirements for Progress in Understanding Solar Flare Energy Transport: The Impulsive Phase

A white Paper in response to the ***Solar and Space Physics (Heliophysics) Decadal Survey***

Graham S. Kerr[1,2]

graham.s.kerr@nasa.gov; kerrg@cua.edu

Co-Authors:

Meriem Alaoui[2,3], Joel C. Allred[2], William Ashfield[4], Thomas Y. Chen[5], Brian R. Dennis[2], A. Gordon Emslie[6], Lyndsay Fletcher[7,8], Ryan J. French[9], Silvina E. Guidoni[2,10], Fan Guo[11], Laura A. Hayes[12], Hugh S. Hudson[7], Andrew R. Inglis[1,2], Judith T. Karpen[2], Adam F. Kowalski[13,9], Ryan O. Milligan[14], Shaun McLaughlin[14], Aaron Monson[14], Vanessa Polito[4], Jiong Qiu[15], Daniel F. Ryan[16], Albert Y. Shih[2]

(1) The Catholic University of America, (2) NASA/GSFC, (3) University of Maryland, (4) Bay Area Environmental Research Institute, (5) Columbia University, (6) Western Kentucky University, (7) University of Glasgow, (8) University of Oslo, (9) National Solar Observatory, (10) American University, (11) Los Alamos National Laboratory, (12) European Space Agency, (13) University of Colorado at Boulder, (14) Queens University Belfast, (15) Montana State University, (16) FNHW University of Applied Sciences.

Summary:

Solar flares are a fundamental component of solar eruptive events (SEEs), along with solar energetic particles (SEPs) and coronal mass ejections (CMEs). Flare emission is the first component of a SEE to impact the Earth's ionosphere which can set the stage for the later effects of the space weather event. Magnetic reconnection drives SEEs by restructuring the solar coronal magnetic field, liberating a tremendous amount of energy which is partitioned into various physical manifestations: particle acceleration, mass and magnetic-field eruption, atmospheric heating, and the subsequent emission of radiation as solar flares. In this white paper we discuss the observational and theoretical advances required in order to make substantial progress in understanding the physical processes acting during the impulsive phase of a flare. That is, the initial rapid and intense period in which a tremendous amount of energy is released over the span of several minutes, resulting in the dramatic broadband increase to the solar radiative output. A second white paper by us covers the flare's gradual phase, that is the decay phase where processes occur over longer timescales.

1 Overview

Solar flares are a fundamental component of solar eruptive events (SEEs), along with solar energetic particles (SEPs) and coronal mass ejections (CMEs). Electromagnetic radiation from the flare is the first component of the SEE to impact Earth's atmosphere and can set the stage for any space weather event to follow. Magnetic reconnection drives SEEs by restructuring the solar coronal magnetic field, liberating a substantial portion of stored magnetic energy, partitioned into various physical manifestations [e.g. 1, 2]. To understand, explain, and ultimately predict geoeffective solar flare events, the heliophysics community requires a comprehensive understanding of the processes that transform and distribute stored magnetic energy on the Sun into other forms, including the broadband radiative enhancement that characterizes flares.

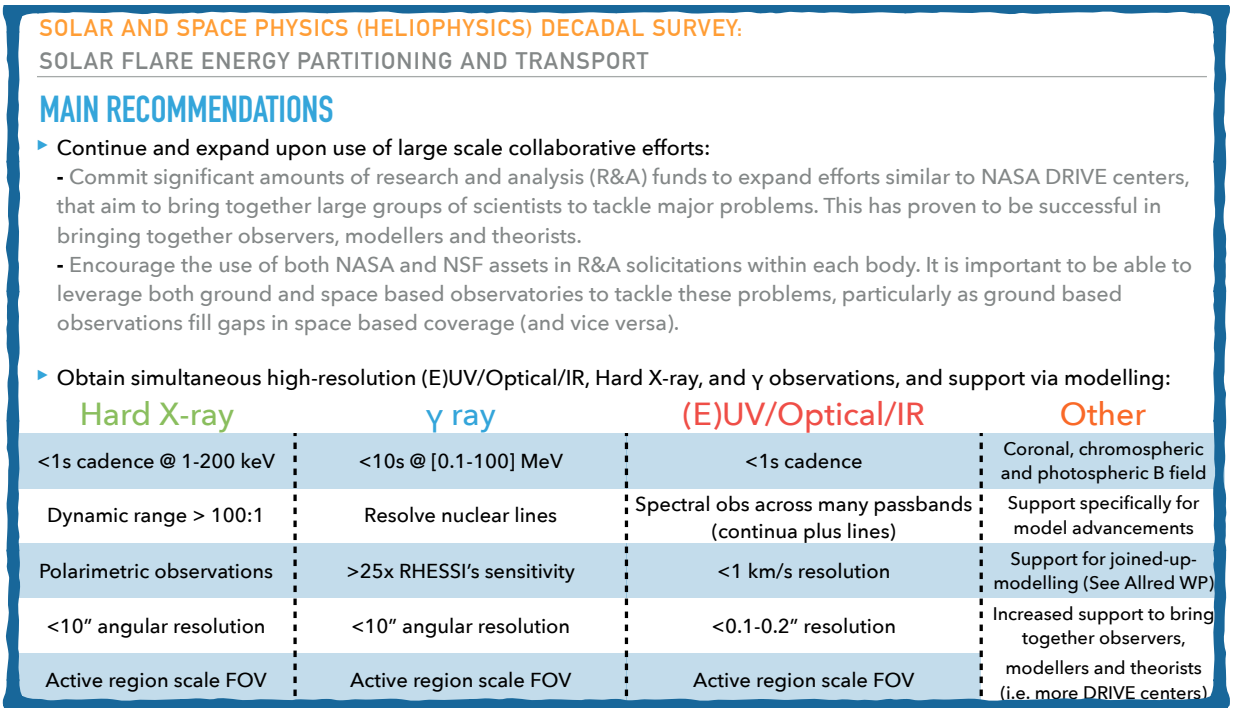

Figure 1: *Our main recommendations for making progress on understanding energy transport and partitioning during the impulsive phase of solar flares.*

This white paper presents a general overview of energy transport during the impulsive phase of flares: the rapid and intense increase of the solar radiative output immediately following the onset of the magnetic reconnection that also creates the CME. Looking ahead, we also discuss prospects for obtaining deeper insights into this important phenomenon. Our approach to solar flare research over the next decade, summarized in Figure 1, is driven by the following needs:

(1) to identify the sites of energy release and particle acceleration in the solar atmosphere;

(2) to characterize in space and time the most energetically important components;

(3) to understand how energy is transported and dissipated into heating and driving mass motions in the Sun's atmosphere, spanning the photosphere to the corona.

Coordinated observations before, during, and after a solar flare event can characterize the

magnetic fields, plasma density, temperature, flow velocities, wave fields, and the spectra and directivity of flare-accelerated electrons and ions. These properties should be measured as close (both in space and in time) to the release site as possible, to minimize the effects associated with transport and propagation. While we must determine the acceleration mechanism(s) responsible for acceleration of electrons and the physical effects (collisions, waves, return currents) that affect their transport, we must also push beyond the standard paradigm of energy transport principally via electron beams, in particular by addressing the extent to which flare-accelerated ions, Alfvén waves, and direct heating in the reconnection region, contribute to the transport of energy from the primary energy release site in the corona throughout the entire flare volume, spanning different regions of the solar atmosphere. To determine the extent to which models accurately account for the wide range of observed flare phenomena, we must confront them with pertinent observations of the highest quality. Our overarching goal is to develop theories that can reproduce fundamental and universal observational features of flares, and to use observations to drive improvements in the included physics in cases where existing models fail to adequately account for observed characteristics.

2 NONTHERMAL ELECTRONS

Flare-accelerated nonthermal electrons have long been thought to be a primary means by which energy is transported through the flaring atmosphere. Although great strides have been made, both observationally and theoretically, in our understanding of the role of flare-accelerated electrons in energy transport, the following fundamental questions remain largely unanswered: (1) where and on what time scales are electrons accelerated? (2) what are their energy and angular distributions? (3) what governs the propagation of accelerated electrons from a coronal acceleration site toward the chromosphere and into interplanetary space?; and (4) what effects do these electrons have on the ambient medium in which they propagate?

These questions persist in part due to the current observational limitations of hard X-ray (HXR) and microwave emission - the principal signatures of electron acceleration. In particular, present HXR observations lack the dynamic range required to effectively sample the relatively weak radiation from the corona in the presence of the much brighter footpoint emission from the chromosphere. High-cadence, arcsecond HXR imaging spectroscopy, with the dynamic range necessary to simultaneously image (and thus spatially separate) both strong and weak sources, is required. It is particularly crucial to resolve coronal emission from both trapped and propagating/precipitating electrons, chromospheric sources, the more extended thermal sources above the footpoints, and the indirect albedo source from photospherically-scattered primary photons. This is necessary to better discern the energy flux delivered to the chromosphere, to better determine the spectral flattening and cutoff at low energies (if it exists), and to test models of electron acceleration and propagation.

To address these issues requires observations of the HXR spectrum (and associated context observations in the EUV and soft X-ray bands) with spatial and temporal resolutions compatible with the distances and times over which electrons lose (and possibly gain) energy. Radio observations also offer diagnostics of the higher-energy component of the accelerated electron

spectrum and characterize the magnetic field environment in which acceleration and propagation occurs. While RHESSI-era [3] HXR observations have made substantial progress in this area, their temporal resolution was limited by the 4-second time spacecraft rotation interval required to adequately cover the phase space ("visibilities") to produce a scientifically valuable image. The use of focusing optics for HXR instrumentation, would provide the desired dynamic range, spatial and temporal resolutions, alleviating this problem and would allow very significant advances in our knowledge of the HXR radiation field, and hence of the physical characteristics (spectrum, angular distribution, time variation) of the electrons that produce it.

Electron acceleration. Several electron acceleration mechanisms have been proposed, which differ substantially in the locations, spatial and temporal scales, and physical processes involved. Candidates include acceleration by large-scale electric fields at reconnection sites (e.g., [4]), contracting [5, 6] or merging magnetic islands along the current sheet [7, 8], reconnection outflow jets [9], termination shocks [10, 11], stochastic acceleration at the top of flare arcades [12], and parallel electric fields produced by kinetic Alfvén waves [13]. Establishing the locations, temporal evolution, spectra and directivity characteristics of HXR sources (both coronal and footpoint) through, e.g., stereoscopic observations from a suite of spacecraft (which could individually be very straightforward and inexpensive to produce) can discriminate among these possibilities. Polarization measurements are also an extremely valuable diagnostic, but to be effective must also be made with arcsecond spatial resolution in order to mitigate the effects of source inhomegeneity on the overall polarization state.

Electron propagation and energy deposition. Many factors affect the transport of electrons from the acceleration region and the associated energy deposition profile, and these can be manifested in subtle HXR spectral features. There have been notable successes in efforts to explain the such features in terms of electron acceleration [14] and propagation [15, 16] models. For example, it has been shown that effects such as nonuniform ionization [17, 18] and strong anisotropy of the electron or X-ray directivity [19] can account for relatively gentle breaks in the photon spectrum. However, stronger breaks, which can be observed in large flares, are more difficult to explain [20, 21]. To make progress discriminating between spectral features associated with acceleration and propagation processes requires high spectral and temporal resolution (~ 1 s) X-ray observations over an energy range at least up to 200 keV, with a dynamic range ($> 100:1$) sufficient to accurately characterize both coronal and chomospheric emission regions. Imaging spectroscopy of the thermal plasma permits differentiation among candidate mechanisms for creating hot coronal plasma, including direct heating [22] in or near the reconnection region; energy loss of accelerated electrons through Coulomb collisions and Ohmic dissipation of the beam-neutralizing return current; and ablation ("evaporation") of heated chromospheric material [23]. Electron transport models are used to interpret X-ray and microwave spectra, which provide valuable, complementary, information on the electron distribution, and to drive radiation-hydrodynamic simulations. Hence such models must evolve to self-consistently incorporate not only Coulomb collisions, but also return currents, magnetic mirroring, synchrotron radiation [24], wave-particle interactions [25] and non-Maxwellian *ambient* electron distributions [26]. In Figure 2 we show synthetic EUV and HXR observations obtained from a flare

radiation-hydrodynamic model (cf. [27]). The nonthermal electron distributions were tracked through the simulation to predict the HXR emission that would be observed. The wide range of HXR intensities throughout the flare volume compellingly demonstrates the need for high dynamic-range HXR imaging spectroscopy in concert with high resolution (E)UV data.

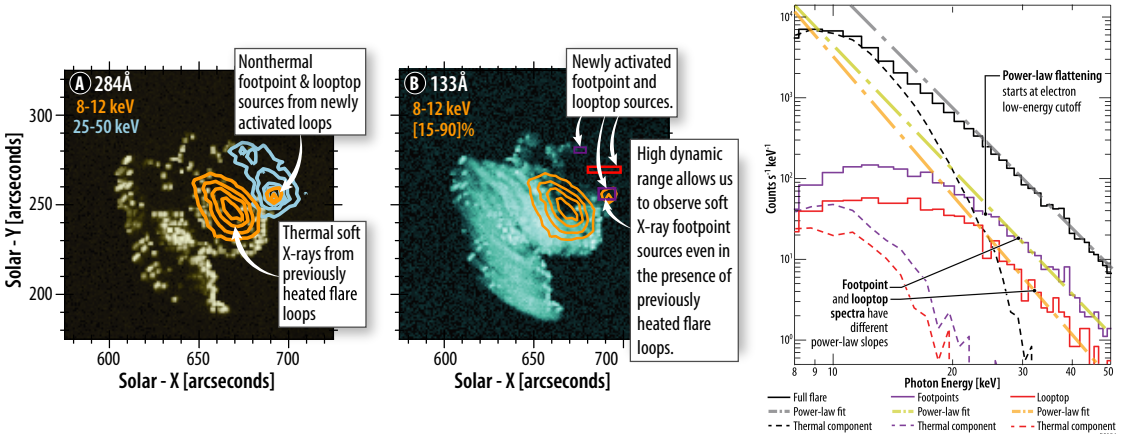

Figure 2: *A simulation showing the value of high-dynamic-range HXR observations. Panels (A) and (B) show X-ray observations upgraded to what might be detected by a sensitive imager with high dynamic range, overlaid on synthetic EUV images. Weak sources are observable even in the presence of more intense sources. Panel (C) shows spectra from the full flare (black), footpoints (purple) and looptop (red) sources, as indicated by the colored boxes in panel (B). The difference in spectra between looptop and footpoint sources is a diagnostic of transport effects.*

Anisotropy in the accelerated electron population, a hallmark of many acceleration models [28], can be determined by stereoscopic observations of HXR directivity — HXR spectral observations of a flare from two different viewpoints. Anisotropy can also be evaluated from X-ray polarimetry with improved sensitivity [29]. Radio observations yield additional information about the anisotropy of the electron distribution at $\gtrsim$200 keV and the magnetic field strength, both essential components of acceleration and propagation mechanisms.

The magnetic reconnection process that energizes flares also generates magnetic forces that drive CMEs. Although downward-directed accelerated electrons and their radiative output have been studied intensely for decades, the upward-driven counterparts have received relatively little attention. Those electrons penetrate the magnetic flux rope that comprises the CME, and may be released into the heliosphere as solar energetic particles [30]. To separate the downward and upward propagating electron populations in SEEs and understand their relationship, we need sensitive HXR and microwave imaging spectroscopy with high dynamic range because the escaping electron flux is weaker compared to flare footpoints.

Once electrons reach the chromosphere and transition region, they rapidly heat (and ionize) the plasma, and drive strong mass flows. The spatio-temporal evolution of chromospheric flare sources, observed in the (E)UV/optical/IR spectral ranges, can be used to determine footpoint source areas, and hence calculate the electron energy *flux* from the total electron *rate* deduced from HXR observations, and their spectral properties can be used to determine the thermodynamic state of the plasma. Variations in the flare emission across the electromagnetic spectrum are common and often quasi-periodic [31]. The origin of these quasi-periodic pulsations (QPPs) is unknown, but they are probably related to intermittent energy release and particle acceleration

processes (e.g., bursty reconnection). QPPs have also been observed in HXRs (e.g., [32]), but we are reaching a limit in our ability to detect short period (on the order of seconds) QPPs. Because many EUV images lack sufficient cadence and are typically saturated during flares, we have been unable to localize QPPs and hence constrain their driving mechanism. To ensure that we are able to detect the rapid thermodynamic response to precipitating nonthermal electrons, and to unlock the diagnostic properties of QPPs, we must have unsaturated (E)UV/optical/IR observations with sub-second temporal resolution and sub-arcsecond spatial resolution, covering a wide temperature range.

3 Nonthermal Ions

Most research into flare-accelerated particles has centered around nonthermal electrons. However, ions (protons, and, to a lesser extent, α particles and other heavier ions) are also accelerated in flares [33–35], and may well carry as much energy as the energetic electrons [1, 2]. Neglecting nonthermal ions in flare models means that *we are potentially ignoring up to half of the flare energy transported through the Sun's atmosphere.* A significant theoretical and observational effort in the next decade is crucial to fill this gap in our understanding.

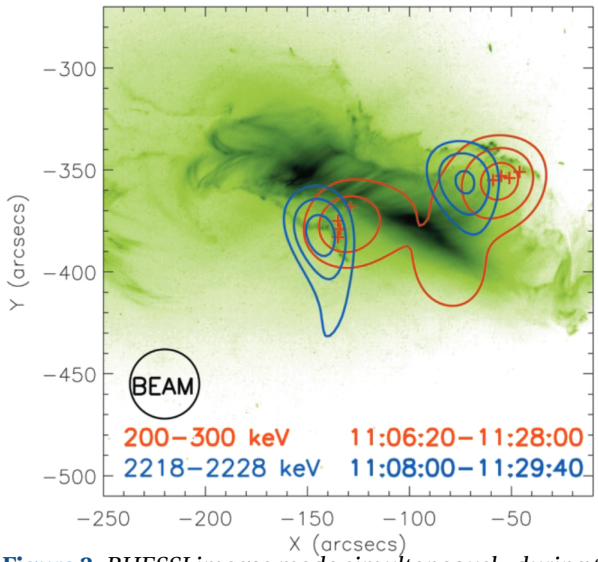

Figure 3: *RHESSI images made simultaneously during the October 28 2003 flare in two different energy ranges. A significant offset is evident between the double γ-ray sources (2218 - 2228 keV) produced by energetic ions and the HXR sources (200-300 keV) produced by energetic electrons. This could point to different transport effects and/or acceleration mechanisms of the different responsible particles [36]. Additional imaging observations in γ rays and HXRs are required, over a range of flare magnitudes, to shed light on the relation between accelerated electrons and ions in solar eruptive events. Figure from [37].*

Flare-accelerated protons have received less attention partly because of the difficulty in detecting their (nuclear) γ-ray signatures; this is especially true for low-energy ions that may carry most of the energy and do not generate a γ-ray signature. The resulting lack of constraints on this spectral range have led to a relative dearth of theoretical studies. While we advocate for more γ-ray observations, we also point out that atmospheric response codes can be used, in combination with EUV and soft X-ray diagnostic observations, to establish a plausible range of nonthermal proton beam properties and mechanisms (e.g., energy loss, scattering by wave-particle interactions [e.g., 38]) that modify the ion particle distribution.) For example, observations from the lower solar atmosphere, where proton beams can penetrate to but electrons cannot [24, 39, 40], can be compared to synthetic observables from simulations driven by electron, proton, or mixed-species beams. The most prominent example is white-light flares (WLFs), which are enhancements to the optical continuum whose origin has long been debated [e.g., 39, 41]. There is evidence that WLFs are produced in the photosphere [39, 41–43], though

insufficient power is carried by the highest energy electrons able to penetrate to the deepest atmospheric layers. Spectroscopy [44] and sunquakes [45, 46] have identified other signatures of energy deposition into the deepest layers in some large flares. Clearly an alternative agent capable of penetrating to deep layers is required. Proton beams are a prime candidate, so emission from these regions can provide valuable diagnostics on proton acceleration and propagation.

Directly establishing the total energy in accelerated ions, the energy spectrum of those ions, and their spatiotemporal relation to flare accelerated electrons, is the best way to constrain acceleration models and drive flare heating models. For ions > 1 MeV, these properties can be determined from γ-ray observations, e.g., nuclear de-excitation lines between 1 – 10 MeV, the 2.223 MeV neutron-capture line, the positron-annihilation line at 511 keV, and the weak radiative capture lines [47] that are produced by relatively low-energy protons. Observations to energies in excess of 100 MeV can probe pion-decay emission (a broad line peaking at 70 MeV), constraining the flux and spectral distribution of the highest energy ions. A sensitivity at least twice that of RHESSI is required to observe γ-rays from M-class events with sufficient spatial resolution to determine the location of chromospheric γ-ray footpoints relative to HXR footpoints and hence to address the open question of whether they are separated (as has been suggested by prior observations [37]), or co-located, which has direct implications for acceleration models. Figure 3 shows a rare example in which γ-ray and HXR observations were imaged cotemporally by RHESSI, showing the γ-ray and HXR footpoints offset from each other by ~20 arcsec. This could mean that the ions and electrons originate from different acceleration mechanisms [36] or undergo different transport effects. Additional simultaneous observations of X-rays and γ-rays < 10 keV to > 100 MeV are required to further address this relation between electrons and ions.

Flare-accelerated protons < 1 MeV can also be revealed by nonthermal Lα (or Lβ) wing asymmetries that carry information about the flux, energy spectrum, and direction of the incident protons [48]. These emissions are produced by nonthermal protons that capture an electron from a neutral hydrogen atom (charge exchange), yielding an excited neutral hydrogen atom that subsequently emits a Doppler-shifted Lα photon.

Downward-directed protons that charge-exchange on ambient hydrogen thus produce a red-wing enhancement, and upward-directed protons yield a blue-wing enhancement. This signature has not yet been observed on the Sun, largely due to the paucity of Lα flare observations, but has been observed during a stellar flare [49]. A similar effect has been observed in terrestrial aurorae [50] and is being used to understand solar wind interactions within the Martian atmosphere to produce proton aurorae [51]. However, a search for asymmetries in the wings of He II 304 Å, caused by charge exchange with nonthermal α-particles, failed to detect this effect [52], although existing theoretical studies predict that it should have been detectable. The estimated intensity of these signatures must be revised by codes capable of modelling the time-dependent, propagating ion distributions in an atmosphere with realistic ionization stratification.

4 Alfvén Waves

Magnetohydrodynamic (MHD) waves are undoubtedly produced in the corona during the large-scale restructuring of the magnetic field during flares [e.g., 53–57]. Downward-propagating

Alfvén waves may heat the lower atmosphere via Joule dissipation of the associated currents [e.g., 58], ion-neutral friction [e.g., 59], or turbulent dissipation [e.g., 60]. Energy transport by Alfvén waves is well established in the magnetosphere [see reviews in 61, 62], but their role in solar flare energy transport remains unclear. The possibility that a non-trivial amount of the flare energy could reside in Alfvén waves demands further exploration.

High-frequency ($f \gtrsim 1$ Hz, required for the waves to penetrate the steep transition region density gradient [59]) downward-propagating Alfvén waves have received renewed attention as a potential means to transport energy from the coronal energy-release site to the chromosphere or deeper [59, 63], and even as a means to accelerate electrons locally in the chromosphere [63]. Waves of different frequency heat different locations in the atmosphere, depending on the ionization stratification, and several numerical experiments [64–66] have demonstrated that Alfvén waves could indeed efficiently heat the chromosphere and temperature-minimum region producing mass flows consistent with observations. However, the lack of definitive observational constraints on wave parameters has severely hampered efforts to make further progress.

In the long term, we should aim to develop a full radiative MHD flare simulation capable of resolving Alfvén wave transport and dissipation and incorporating nonthermal particles. Radiative MHD simulations of flares must be augmented to include an accurate Non Local Thermodynamic Equilibrium (NLTE) chromosphere. However, a simulation that fully resolves the required spatial scales (down to meters in some situations) represents a challenge that may not be fully realized before 2050. To make progress on this question in the next decade, we should start with improvements to existing radiation hydrodynamic models, for example by implementing more realistic wave spectra and propagation processes.

Observational efforts should focus on measuring the properties of these high-frequency waves in the chromosphere, determining where they originate and where they deposit their energy. This will require high cadence (sub-second) and high spatial resolution (less than 0.1 arcsec) spectroscopy of both the chromosphere and corona. Measurements of nonthermal line broadening from spectral lines observed at a series of heights can be used to estimate the energy flux carried by the propagating waves [e.g., 67, 68]. Further, because the waves take several seconds to propagate through the chromosphere, emission at increasing depths should switch on sequentially. The amount of energy carried by the waves depends on the magnetic-field perturbation, requiring coronal magnetic-field fluctuations to be measured to the level of a few percent. The height dependence of the magnetic field and density stratification define the all-important Alfvén speed, and even a coarse observational sampling of the field strength at different heights, which could potentially be provided by DKIST,could lead to major breakthroughs.

Here, the flare community would benefit from closer collaboration with our magnetospheric colleagues. The generation, propagation, and dissipation of Alfvén waves in the magnetosphere is a well-established research field [61, 62] that benefits from *in-situ* measurements. Although the characteristic plasma scales and collisionality of the solar atmosphere and the magnetosphere differ substantially, for the most part integration of these research efforts would greatly advance our understanding of energy partitioning between particle acceleration and wave generation, the energy spectrum of Alfvén waves, and the role of pertinent wave-particle interactions.

REFERENCES

[1] Emslie, A. G., et al. 2012, ApJ, 759, 71, doi:10.1088/0004-637X/759/1/71
[2] Aschwanden, M. J., et al. 2017, ApJ, 836, 17, doi:10.3847/1538-4357/836/1/17
[3] Lin, R. P., et al. 2002, Sol. Phys., 210, 3, doi:10.1023/A:1022428818870
[4] Benka, S. G. & Holman, G. D. 1994, ApJ, 435, 469, doi:10.1086/174829
[5] Guidoni, S. E., et al. 2016, ApJ, 820, 60, doi:10.3847/0004-637X/820/1/60
[6] Guidoni, S. E., et al. 2022, ApJ, 925, 191, doi:10.3847/1538-4357/ac39a5
[7] Drake, J. F., et al. 2013, ApJL, 763, L5, doi:10.1088/2041-8205/763/1/L5
[8] Arnold, H., et al. 2021, Physics Review Letters, 126, 135101, doi:10.1103/PhysRevLett.126.135101
[9] Che, H., et al. 2021, ApJ, 908, 72, doi:10.3847/1538-4357/abcf29
[10] Mann, G., et al. 2006, A&A, 454, 969, doi:10.1051/0004-6361:20064990
[11] Kong, X., et al. 2019, ApJL, 887, L37, doi:10.3847/2041-8213/ab5f67
[12] Miller, J. A., et al. 1996, ApJ, 461, 445, doi:10.1086/177072
[13] Zharkova, V. V., et al. 2011, Space Science Rev., 159, 357, doi:10.1007/s11214-011-9803-y
[14] Grigis, P. C. & Benz, A. O. 2008, ApJ, 683, 1180, doi:10.1086/589826
[15] Battaglia, M. & Benz, A. O. 2008, A&A, 487, 337, doi:10.1051/0004-6361:200809418
[16] Su, Y., et al. 2011, ApJ, 731, 106, doi:10.1088/0004-637X/731/2/106
[17] Kontar, E. P., et al. 2003, ApJL, 595, L123, doi:10.1086/378172
[18] Su, Y., et al. 2009, ApJ, 705, 1584, doi:10.1088/0004-637X/705/2/1584
[19] Massone, A. M., et al. 2004, ApJ, 613, 1233, doi:10.1086/423127
[20] Alaoui, M. & Holman, G. D. 2017, ApJ, 851, 78, doi:10.3847/1538-4357/aa98de
[21] Alaoui, M., et al. 2019, Sol. Phys., 294, 105, doi:10.1007/s11207-019-1495-6
[22] Longcope, D. W., et al. 2009, ApJL, 690, L18, doi:10.1088/0004-637X/690/1/L18
[23] Holman, G. D. 2016, JGR (Space Physics), 121, 11,667, doi:10.1002/2016JA022651
[24] Allred, J. C., et al. 2020, ApJ, 902, 16, doi:10.3847/1538-4357/abb239
[25] Hannah, I. G., et al. 2013, A&A, 550, A51, doi:10.1051/0004-6361/201220462
[26] Alaoui, M., et al. 2021, ApJ, 917, 74, doi:10.3847/1538-4357/ac0820
[27] Kerr, G. S., et al. 2020, ApJ, 900, 18, doi:10.3847/1538-4357/abaa46
[28] Jeffrey, N. L. S., et al. 2020, A&A, 642, A79, doi:10.1051/0004-6361/202038626
[29] Casadei, D., et al. 2017, A&A, 606, A2, doi:10.1051/0004-6361/201730629
[30] Masson, S., et al. 2013, apj, 771, 82
[31] Zimovets, I. V., et al. 2021, Space Science Rev., 217, 66, doi:10.1007/s11214-021-00840-9
[32] Knuth, T. & Glesener, L. 2020, ApJ, 903, 63, doi:10.3847/1538-4357/abb779
[33] Ramaty, R. & Mandzhavidze, N. 2000, in Amer. Inst. of Phy. Conf.Series, Vol. 522, 401–410
[34] Shih, A. Y., et al. 2009, ApJL, 698, L152, doi:10.1088/0004-637X/698/2/L152
[35] Zhang, Q., et al. 2021, Physics Review Letters, 127, 185101, doi:10.1103/PhysRevLett.127.185101
[36] Emslie, A. G., et al. 2004, ApJL, 602, L69, doi:10.1086/382350
[37] Hurford, G. J., et al. 2006, ApJL, 644, L93, doi:10.1086/505329
[38] Tamres, D. H., et al. 1989, ApJ, 342, 576, doi:10.1086/167617
[39] Neidig, D. F. 1989, SoPh, 121, 261, doi:10.1007/BF00161699
[40] Tamres, D. H., et al. 1986, ApJ, 309, 409, doi:10.1086/164613

[41] Kerr, G. S. & Fletcher, L. 2014, ApJ, 783, 98, doi:10.1088/0004-637X/783/2/98
[42] Hiei, E. 1982, SoPh, 80, 113, doi:10.1007/BF00153427
[43] Watanabe, K., et al. 2013, ApJ, 776, 123, doi:10.1088/0004-637X/776/2/123
[44] Metcalf, T. R., et al. 1990, ApJ, 350, 463, doi:10.1086/168400
[45] Kosovichev, A. G. & Zharkova, V. V. 1998, Nat, 393, 317, doi:10.1038/30629
[46] Zharkova, V. & Zharkov, S. 2015, Sol. Phys., 290, 3163, doi:10.1007/s11207-015-0813-x
[47] MacKinnon, A. L. 1989, A&A, 226, 284
[48] Orrall, F. Q. & Zirker, J. B. 1976, ApJ, 208, 618, doi:10.1086/154642
[49] Woodgate, B. E., et al. 1992, ApJL, 397, L95, doi:10.1086/186553
[50] Ishimoto, M., et al. 1989, GRL, 16, 143, doi:10.1029/GL016i002p00143
[51] Hughes, A., et al. 2019, Journ. Geophys. Res. (Space Phys.), 124, 10,533, doi:10.1029/2019JA027140
[52] Hudson, H. S., et al. 2012, ApJ, 752, 84, doi:10.1088/0004-637X/752/2/84
[53] Kigure, H., et al. 2010, Pub. of the Astron. Soc. of Japan, 62, 993, doi:10.1093/pasj/62.4.993
[54] Birn, J., et al. 2009, ApJ, 695, 1151, doi:10.1088/0004-637X/695/2/1151
[55] Karpen, J. T., et al. 2012, ApJ, 760, 81, doi:10.1088/0004-637X/760/1/81
[56] Kumar, P. & Innes, D. E. 2013, SoPh, 288, 255
[57] Kumar, P., et al. 2017, ApJ, 844, 149
[58] Emslie, A. G. & Sturrock, P. A. 1982, Sol. Phys., 80, 99, doi:10.1007/BF00153426
[59] Russell, A. J. B. & Fletcher, L. 2013, ApJ, 765, 81, doi:10.1088/0004-637X/765/2/81
[60] Ashfield IV, W. & Longcope, D. 2022, *In preparation*
[61] Keiling, A. 2009, Space Science Rev., 142, 73, doi:10.1007/s11214-008-9463-8
[62] Khotyaintsev, Y. V., et al. 2019, Frontiers in Astro. and Space Sci., 6, 70, doi:10.3389/fspas.2019.00070
[63] Fletcher, L. & Hudson, H. S. 2008, ApJ, 675, 1645, doi:10.1086/527044
[64] Reep, J. W. & Russell, A. J. B. 2016, ApJL, 818, L20, doi:10.3847/2041-8205/818/1/L20
[65] Kerr, G. S., et al. 2016, ApJ, 827, 101, doi:10.3847/0004-637X/827/2/101
[66] Reep, J. W., et al. 2018, ApJ, 853, 101, doi:10.3847/1538-4357/aaa2fe
[67] Banerjee, D., et al. 1998, A&A, 339, 208
[68] Oran, R., et al. 2017, ApJ, 845, 98, doi:10.3847/1538-4357/aa7fec